One-Phonon Sideband of Sm^{++} in KBr†

T. TIMUSK* AND M. BUCHANAN‡

Department of Physics, McMaster University, Hamilton, Ontario, Canada

(Received 7 August 1967)

The phonon sideband of the 6890-Å transition of Sm^{++} in KBr is studied. New high-resolution experiments at 7°K are presented, and a theory of the sideband shape is given. It is assumed that the electric field from the phonons is responsible for the sideband, and a detailed shape is calculated by the use of the phonons of pure KBr as determined by neutron measurements. The electric field due to the phonons is calculated by the Ewald method. With the exception of a few peaks that can be attributed to local modes, all the important features of the observed sideband agree with the curve given by the model.

I. INTRODUCTION

THE fluorescence spectrum of Sm^{++} in KBr shows a sequence of very sharp lines extending from 6890 Å to the near infrared. These lines correspond to a transition within the $4f^6$ shell from a $^5D_0$ state to the ^7F levels.[1,2] On the low-energy side of the sharp lines there is a weak continuous spectrum arising from the interaction of the rare-earth ion with the phonons of the host lattice. However, the sideband of the $^5D_0 \rightarrow {}^7F_0$ line at 6890 Å is very distinct. It has been studied by Kaplyanskii and Feofilov[1] and by Bron.[3]

In Sec. II we present a high-resolution photoelectrically recorded spectrum of the sideband at 7°K. A model of the sideband in terms of a long-range electrostatic interaction is given in Sec. IIIA. Section IIIB contains the results of the calculation and comparison with experiment, and in Sec. IIIC we discuss the role of a charge-compensating vacancy. Sidebands of the transition to the $^7F_1$ levels are discussed in Sec. IIID.

II. EXPERIMENTAL RESULTS

The KBr:Sm^{++} crystals were grown in a reducing atmosphere of hydrogen by the Kyropoulos method from a melt of KBr containing 0.5 at.% anhydrous samarium chloride. The emission spectra were measured at 7°K using a Spex $\frac{3}{4}$-m. Czerny–Turner spectrometer with a trialkali photomultiplier. A correction for photomultiplier sensitivity was not made, since it is small and without structure. A 500-W high-pressure mercury lamp was used for excitation.

A recorder trace of the sideband spectrum on the low-energy side of the zero-phonon line at 6890.4 Å is shown in Fig. 1. The spectrum ends abruptly at a frequency of 168 cm^{-1} from the zero-phonon line, which corresponds almost exactly with the highest phonon frequency in KBr. There is also a weak background in the two-phonon region beyond 168 cm^{-1}.

The six large peaks agree well in position with those observed by Kaplyanskii and Feofilov. We have in addition resolved several sharp weak lines in the gap between the acoustical and optical branches. These are possibly local modes from impurities in the KBr. The gap itself agrees quite well in position and width with the gap in pure KBr, but there is a definite small shift towards higher frequencies. The two strong peaks in the acoustical branch have a very striking triangular appearance. These peaks are limited in sharpness by the width of the zero-phonon line, which is 0.7 cm^{-1}. Our instrumental resolution is 0.2 cm^{-1}.

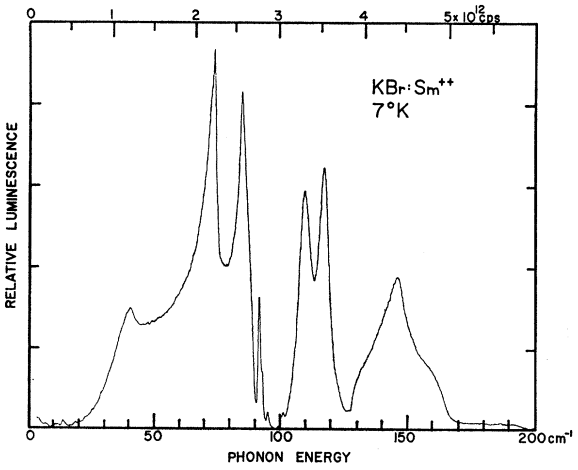

FIG. 1. The sideband on the long-wavelength side of the 6890-Å transition of Sm^{++} in KBr. The curve is a direct recorder trace.

III. THEORY AND DISCUSSION

A. Model for the Sideband

The 6890-Å line is strictly forbidden in cubic symmetry for electric dipole radiation, as it corresponds to a transition between two states of even parity. The presence of electric fields, however, would lower the

† Work supported in part by a grant from the National Research Council of Canada.

* Alfred P. Sloan research fellow.

‡ National Research Council studentship holder.

[1] A. A. Kaplyanskii and P. P. Feofilov, Opt. i Spektroscopiya **16**, 264 (1964) [English transl.: Opt. Spectry. (USSR) **16**, 144 (1964)].

[2] W. E. Bron and W. R. Heller, Phys. Rev. **136**, A1433 (1964).

[3] W. E. Bron, Phys. Rev. **140**, A2005 (1965).

symmetry and make the following transitions possible: the zero-phonon line, arising from the static field from the positive-ion vacancy, which is necessary for electrical neutrality,[2] and the sideband, arising from the time-varying electric field of phonons in the crystal. We have assumed the electric fields to be constant over the samarium ion, and thus are considering a perturbation Hamiltonian of the form $e\mathbf{E}\cdot\mathbf{r}$, where e is the electronic charge, $\mathbf{E}$ is the electric field of the vacancy and the phonons at the samarium site, and $\mathbf{r}$ is the electronic coordinate.[4] The transition probability per unit time, $W_{e\to g}$ is then given by

$$W_{e\to g}=\frac{2\pi}{\hbar}\sum_{\text{final states}}\left|\sum_i\frac{\langle\Psi_g\mid H'+e\mathbf{E}\cdot\mathbf{r}\mid\Psi_i\rangle\langle\Psi_i\mid H'+e\mathbf{E}\cdot\mathbf{r}\mid\Psi_e\rangle}{E_i-E_e}\right|^2\delta(E_g-E_e),\quad(1)$$

where H' is the part of the Hamiltonian giving rise to the optical transition. The Ψ's are total wave functions of the system: Ψ_e is the excited state, Ψ_g the ground state, and Ψ_i an intermediate state. E_e, E_g, and E_i are the energies of these states. The summation on i extends over all odd-parity states.

We have, then, for the phonon sideband transition,

$$W_{e\to g}=\frac{2\pi}{\hbar}e^2\sum_{\text{final states}}\left|\sum_i\frac{\langle 11\Phi_g\mid H'\mid 10\Phi_i\rangle\langle 10\Phi_i\mid\mathbf{E}\cdot\mathbf{r}\mid 00\Phi_e\rangle}{\epsilon_i+\hbar\omega-\epsilon_e}+\frac{\langle 11\Phi_g\mid\mathbf{E}\cdot\mathbf{r}\mid 01\Phi_i\rangle\langle 01\Phi_i\mid H'\mid 00\Phi_e\rangle}{\epsilon_i+\hbar\nu-\epsilon_e}\right|^2$$
$$\times\delta(\epsilon_g-\epsilon_e+\hbar\nu+\hbar\omega),\quad(2)$$

where we have written $\mid\Psi_k\rangle$ as $\mid n_1n_2\Phi_k\rangle$, where n_1 is the number of phonons, n_2 the number of photons, and Φ_k the electronic wave function of the state k of the samarium ion; ϵ_k is now the energy of the electronic level, $\hbar\omega$ the energy of the phonon created, and $\hbar\nu$ the energy of the photon created.

Now $\epsilon_e-\epsilon_g=\hbar\omega+\hbar\nu$, so the denominator of the second term in Eq. (2) may be written as $\epsilon_i-\hbar\omega-\epsilon_g$. We now assume that $\hbar\omega\ll\epsilon_i-\epsilon_e$ and $\hbar\omega\ll\epsilon_i-\epsilon_g$, and obtain terms of the form

$$\sum_i\frac{\langle 11\Phi_g\mid H'\mid 10\Phi_i\rangle\langle 10\Phi_i\mid\mathbf{E}\cdot\mathbf{r}\mid 00\Phi_e\rangle}{\epsilon_i-\epsilon_e}$$
$$+\frac{\langle 11\Phi_g\mid\mathbf{E}\cdot\mathbf{r}\mid 01\Phi_i\rangle\langle 01\Phi_i\mid H'\mid 00\Phi_e\rangle}{\epsilon_i-\epsilon_g}.\quad(3)$$

For a final-state g with the photon polarized along the x direction, one can show, by considering the symmetries of the wave functions and operators, that Eq. (3) gives terms proportional to E_x only.

Finally, we have for transitions involving photons between frequency ν and frequency $\nu+\Delta\nu$ observed in solid angle $\Delta\Omega$ that

$$W_{e\to g}=\frac{\Delta\Omega\nu^3\Delta\nu}{2\pi^2c^3}e^4$$
$$\times\Big|\sum_i\langle\Phi_g\mid r_x\mid\Phi_i\rangle\langle\Phi_i\mid r_x\mid\Phi_e\rangle\big[(\epsilon_i-\epsilon_e)^{-1}+(\epsilon_i-\epsilon_g)^{-1}\big]\Big|^2$$
$$\times E_x^2\delta(\epsilon_g-\epsilon_e+\hbar\nu+\hbar\omega),\quad(4)$$

where $\Delta\nu$ is a constant, and $\hbar\nu^3=(\epsilon_e-\epsilon_g-\hbar\omega)^3\cong(\epsilon_e-\epsilon_g)^3$, a constant, and we have summed over photon polarization, and used $E_x^2=E_y^2$ for cubic symmetry. Hence we have $W_{e\to g}\propto E_x^2$.

The electric field at the samarium site is given by

$$\mathbf{E}=\sum_i{}'Z_ie(\mathbf{u}_0-\mathbf{R}_i-\mathbf{u}_i)/\mid\mathbf{u}_0-\mathbf{R}_i-\mathbf{u}_i\mid^3,\quad(5)$$

where $\mathbf{R}_i$ is the equilibrium position of the ith ion, $\mathbf{u}_i$ its displacement from equilibrium, and Z_ie its charge. The samarium ion has a displacement $\mathbf{u}_0$ from its equilibrium position, which we take as the origin. The summation $\sum'$ extends over all ions except the samarium ion.

Neglecting, for the moment, the existence of the vacancy, and expanding Eq. (5) to lowest order in $\mathbf{u}_i$ and $\mathbf{u}_0$, we have

$$\mathbf{E}=-\sum_i{}'(Z_ie/\mid\mathbf{R}_i\mid^3)\mathbf{u}_i+3\sum_i{}'(Z_ie/\mid\mathbf{R}_i\mid^5)\mathbf{R}_i\cdot\mathbf{u}_i\mathbf{R}_i;\quad(6)$$

the other terms are zero because of cubic symmetry. Then the amplitude of the x component of the electric field on the ion of type κ at the origin, from one phonon of wave vector $\mathbf{q}$ and branch j, is given by

$$E_x(0,\kappa;\mathbf{q},j)=e^{-1}\sum_{\kappa',\beta}\begin{bmatrix}\kappa\kappa'\\ x\beta\end{bmatrix}(1/\sqrt{M_{\kappa'}})$$
$$\times Z_{\kappa'}\xi_\beta(\kappa',\mathbf{q},j)A(\mathbf{q},j).\quad(7)$$

Here κ' is summed over the ions in the unit cell, and over the three cartesian coordinates. The coefficient

$$\begin{bmatrix}\kappa\kappa'\\ \alpha\beta\end{bmatrix}$$

is given by

$$\begin{bmatrix}\kappa\kappa'\\ \alpha\beta\end{bmatrix}=\sum_l\Phi_{\alpha\beta}(l,l';\kappa,\kappa')\exp i\mathbf{q}\cdot(\mathbf{R}_l-\mathbf{R}_{l'}),\quad(8)$$

[4] Our perturbation is not the same as that considered by Bron in Ref. 3. We have used a time-dependent perturbation, as well as the static, on the electronic wave function. Bron has used only the static part to perturb the electronic wave functions, and then assumes the sideband arises from changed overlap of nuclear wave functions. From the experimentally observed two-phonon sideband, one can estimate the contribution from this mechanism. It appears to be less important than that which we have calculated.

where $\Phi_{\alpha\beta}$ is the second derivative of the Coulomb part of the potential

$$\Phi_{\alpha\beta}(l, l'; \kappa, \kappa') = \partial^2\Phi/[\partial u_\alpha(l, \kappa)\partial u_\beta(l', \kappa')]. \quad (9)$$

This coefficient was first introduced by Kellermann, and is best evaluated by the Ewald method.[5] Here $\mathbf{R}_l$ is the position of the lth unit cell. We have used

$$u_\alpha(l, \kappa) = [A(\mathbf{q}, j)/\sqrt{M_\kappa}]\xi_\alpha(\kappa, \mathbf{q}, j)\ \exp i(\mathbf{q}\cdot\mathbf{R}_l - \omega_{qj}t) \quad (10)$$

for the α displacement of the κth ion in the lth unit cell, in the harmonic approximation, for phonon $(\mathbf{q}, j)$. $A(\mathbf{q}, j)$ is the amplitude, $\xi_\alpha(\kappa, \mathbf{q}, j)$ is the α component of the polarization vector, and M_κ is the mass of the κth ion in the unit cell.

At low temperature

$$A(\mathbf{q}, j) = (\hbar/2N\omega_{qj})^{1/2}, \quad (11)$$

and we have

$$E_x(0, 1; \mathbf{q}, j) = e^{-1}\left(\frac{\hbar}{2N}\right)^{1/2}\omega_{qj}^{-1/2}\sum_{\kappa',\beta}\frac{Z_{\kappa'}}{\sqrt{M_{\kappa'}}}\begin{bmatrix}1\kappa'\\ x\beta\end{bmatrix}\xi_\beta(\kappa', \mathbf{q}, j) \quad (12)$$

where 1 refers to the positive ion, for the x component of the electric field on the positive ion at the origin.

B. Calculations and Comparison with Experiment

We have calculated E_x^2 as a function of ω making the following assumptions:

(1) The equilibrium positions of all the ions are those of the pure lattice.

(2) The motions of the ions, including the samarium ion, can be described by the eigenfrequencies and eigenvectors given by the neutron determined shell model of Cowley, Cochrane, Brockhouse, and Woods (model VI),[6] for the pure KBr lattice.

We have obtained the electric field at the samarium site by evaluating Eq. (12) at 64 000 points in the first Brillouin zone, and sorting the contributions to E_x^2 into 100 "bins" ranging from 0 to 167 cm^{-1}. A smooth curve has been drawn through the center point of each contribution in the resultant histogram.

At first, we will include only the electric fields due to the ionic displacement, taking the ionic charge to be unity. A consistent use of the shell model would also include the field from the shells. This we do in the second calculation.

Figure 2 shows the calculated curve for the case of simple ions with no shell field, compared with the experimental curve. The relative scale of the two curves has been chosen arbitrarily.

The calculated curve agrees well with the experimental curve in the relative strengths of the acoustical and optical branches. All the major peaks in the experimental curve are represented. A sharp phonon peak at 132 cm^{-1} in the density of states calculated from the shell model[7] is missing in both calculation and experiment.

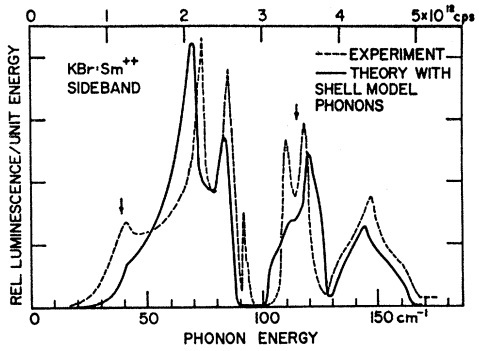

FIG. 2. The theoretical sideband for simple ions compared with the experimental sideband. The arrows indicate local modes observed in $4f^6 \rightarrow 4f^5d$ transitions.

For the purpose of the second calculation, these equations can be extended to include the field from the shells as well. The shells were originally introduced to account for the polarizability of the ions. In our problem their effect is to reduce the electric field due to phonons. Since this reduction is frequency-dependent we have done a detailed calculation of this effect by extending the range of summation in Eq. (5) to run over the shells; $Z_i e$ then refers to the shell charge, and the u's to the shell displacements. The extension of Eq. (12) is similar.

Figure 3 shows the calculation including the shell field. The general effect of including the shells in the calculation is to lower the curve by 18% in the acoustical branch and by 45% in the optical branch. The main features are otherwise unchanged. In the transverse optical branch the inclusion of the shell field gives a double peak, much as we observe.

There remain several discrepancies between both calculations and the experiment. First, there are the sharp peak in the gap at 92 cm^{-1} and the strong peak at 41 cm^{-1} in the experimental curves not appearing in the theory. Also the peak at 111 cm^{-1} is much weaker in the first calculation than that observed. The peak in the gap may be a local mode of an impurity, and the 41 cm^{-1} is probably a local-mode vibration associated with the samarium. Its position agrees well with a local mode observed by Wagner and Bron at 39 cm^{-1} in the absorption spectrum of a $4f^6 \rightarrow 4f^5d$ transition of KBr:Sm^{++}.[8] These authors also observed a local mode at 115 cm^{-1}. This mode may be responsible for the discrepancies in our calculations in the transverse optical region.

Secondly, our calculated frequencies are too low,

[5] E. W. Kellermann, Phil. Trans. Roy. Soc. (London) **238**, 513 (1940).

[6] R. A. Cowley, W. Cochrane, B. N. Brockhouse, and A. D. B. Woods, Phys. Rev. **131**, 1030 (1963).

[7] E. R. Cowley and R. A. Cowley, Proc. Roy. Soc. (London) **A292**, 209 (1966).

[8] Max Wagner and W. E. Bron, Phys. Rev. **139**, A223 (1965).

since we have used the shell model at 90°K, while the experiment was done at 7°K. The use of a model correct at low temperature would improve the agreement in the positions of the gap and the end of the spectrum, as well as many of the peaks. The peak predicted at 70 cm^{-1}, however, is probably shifted more than what can be attributed to a temperature effect.

We cannot on the basis of our experiments conclude which of the two calculations best fits the data. The simple ion calculation gives a better distribution of intensities whereas the inclusion of the shell field improves the shape of the TO branch. It is difficult to take the shell field literally since some of the parameters of the shell model have physically unrealistic values. Our simple ion calculation may be the best description until a more physical model is developed. It must be emphasized, however, that even for the simple ion calculation, we have used the ionic displacements given by the *complete* shell model.

C. Effect of the Vacancy

The vacancy, which we assume to be in the second neighbor position at 110, in agreement with the experimental work of Bron and Heller,[2] has very little effect from the point of view of the sideband. We have carried out a calculation similar to the one outlined above, including several extra terms in Eqs. (5) to (12) to take into account the vacancy.

In this case Eq. (5) becomes

$$\mathbf{E}=\sum_i{}' \frac{Z_i e(\mathbf{u}_0-\mathbf{R}_i-\mathbf{u}_i)}{|\mathbf{u}_0-\mathbf{R}_i-\mathbf{u}_i|^3}-\frac{e(\mathbf{u}_0-\mathbf{R}_v-\mathbf{u}_v)}{|\mathbf{u}_0-\mathbf{R}_v-\mathbf{u}_v|^3}, \quad (13)$$

where $\mathbf{R}_v$ is the equilibrium position of the missing ion, and $\mathbf{u}_v$ its displacement. This leads to, for the x component of the electric field from the vacancy and all the phonons,

$$E_x(0,1)=\frac{e}{|\mathbf{R}_v|^3}R_{vx}+\left(\frac{\hbar}{2N}\right)^{1/2}\sum_{\mathbf{q},j}\omega_{\mathbf{q}j}^{-1/2}$$
$$\times\left\{\frac{1}{e}\sum_{\kappa',\beta}\left(\begin{bmatrix}1\kappa'\\ x\beta\end{bmatrix}\Big/\sqrt{M_{\kappa'}}\right)\xi_\beta(\kappa',\mathbf{q},j)\right.$$
$$+\frac{e}{|\mathbf{R}_v|^5}\frac{[\exp(i\mathbf{q}\cdot\mathbf{R}_v)-1]}{\sqrt{M_1}}$$
$$\left.\times\sum_\beta(|\mathbf{R}_v|^2\delta_{x\beta}-3R_{vx}R_{v\beta})\xi_\beta(\kappa,\mathbf{q},j)\right\}. \quad (14)$$

In this case we must average over all possible positions of the vacancy because of the lower symmetry. The resultant spectrum differs from that shown in Fig. 2 only in very small changes of much less than 1% in the relative intensities of the peaks.

The vacancy gives a static electric field at the samarium site, given by $\mathbf{E}=(e/|\mathbf{R}_v|^3)\mathbf{R}_v$. This static field gives rise to the zero-phonon line. We can thus predict the ratio of the intensity of the one-phonon sideband to the intensity of the zero-phonon line. The ratio for the first calculation (simple ions), I_1/I_0, is 0.06, which is 15% of the experimentally determined value of 0.40. However, the shifts in the equilibrium positions have not been taken into account; it is obvious that the intensity of the calculated zero-phonon line will be reduced by dielectric effects due to polarization of the lattice by the long-range dipole field of the samarium ion and vacancy. Also, the intensity as calculated is dependent on all samarium ions having a vacancy as their second nearest neighbor; ions with no vacancy would give no contribution, and ions with a vacancy as fourth nearest neighbor a much smaller contribution. We expect that a more realistic calculation taking these effects into consideration, would give a much reduced zero-phonon line and bring the strength of the sideband relative to the zero-phonon line into better agreement with experiment. We think, therefore, that the major portion of the sideband can be attributed to the process described here.

D. Other Sidebands

Sidebands associated with the $^5D_0 \rightarrow {}^7F_1$ transitions have also been observed. The $^7F_1$ level is split into three components at 7016.0, 7032.2, and 7042.7 Å by the crystal field.[1] The sidebands here overlap, are more difficult to observe, and appear to contain several unidentified sharp lines probably due to impurities. Detailed analysis is difficult, but the main features are consistent with the results for the $^7F_0$ sideband, and several of the strong peaks seen in the $^7F_0$ sideband can be identified here also.

IV. DISCUSSION

The peaks and corners visible in the sideband spectrum can be identified as Van Hove singularities in the dispersion curves of KBr. These features agree in the calculated curve and in the measured curve to within 1 or 2%, with the notable exception of the peak at 74 cm^{-1} in the experimental curve, which the calculation predicts at 70 cm^{-1}.

The location of these singularities in wave vector space has been determined by searching through dis-

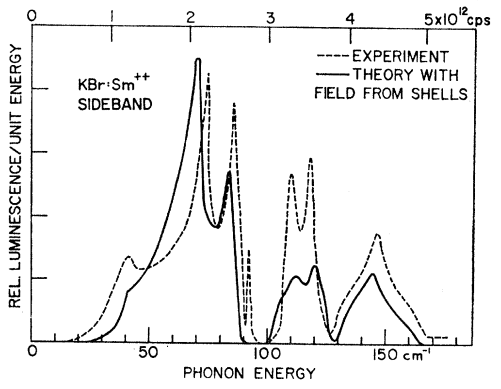

FIG. 3. The theoretical sideband for ions with shells compared with the experimental sideband.

persion curves (calculated using the shell model) for regions of zero gradient. Many of the critical points are found to occur for wave vectors in high symmetry directions.

Exceptions, however, are the high peak at 70 cm^{-1}, the peak at 83 cm^{-1}, and the peak at 132 cm^{-1} in the density of states which is missing in the sideband. These arise from saddle points located in off symmetry directions, in the planes $(1\bar{1}0)$, (001), and $(01\bar{1})$, respectively.

The discrepancy of the peak at 74 cm^{-1} is 6% greater than the errors in our measurement and the effects due to temperature. It may arise from distortion of the crystal or from the long-range strain field caused by the samarium ion and its associated vacancy. However, in view of the fact that the singularity involved arises from the off-symmetry dispersion curves, and has not been measured directly in the neutron work, we cannot exclude the possibility that the shell-model prediction of the frequency of this peak may be in error.

The major remaining problem seems to be the calculation of the contribution of the distortions of the ions to the electric field. Further refinements of the shell model, such as the "breathing shell model",[9] may give a better description of the field than the simple shell model used here.

In summary, we conclude that a good description of the sideband of the 6890-Å samarium transition can be obtained from a long-range electrostatic interaction using phonons of the pure lattice. Agreement between calculation and experiment is good and hence the effect of local perturbations such as mass and force constant changes, while present, are small.

ACKNOWLEDGMENT

We would like to thank Dr. E. J. Woll, Jr. for numerous helpful discussions.

[9] U. Schroeder, Solid State Commun. **4**, 347 (1966).

PHYSICAL REVIEW VOLUME 164, NUMBER 2 10 DECEMBER 1967

Density Effect for the Ionization Loss of Charged Particles. II*

R. M. STERNHEIMER
Brookhaven National Laboratory, Upton, New York
(Received 7 June 1967)

The reduction in the ionization loss of charged particles due to the polarization of the medium (density effect) has been evaluated for several additional substances, in particular for $Li_2B_4O_7$, Al_2O_3, CaF_2, NaI, CsI, lithium aluminosilicate glass, and a H_2-Ne mixture used in bubble chambers.

THE density effect correction for the ionization loss of charged particles[1–6] has been previously evaluated for various substances.[4–6] The purpose of the present paper is to give the results of additional calculations for the following materials: LiF, $Li_2B_4O_7$, Al_2O_3, lithium aluminosilicate glass, CaF_2, NaI, CsI, a H_2-Ne mixture used in bubble chambers, and a plastic scintillator (N.E.-102). We shall also make some suggestions concerning useful quantities which could be tabulated to facilitate the calculation of the most probable energy loss ϵ_{prob} in a sample of thickness t.

The procedure of the calculation of the density effect followed the same lines as in Ref. 4–6. The calculated values of δ have been expressed in the form

$$\delta=4.606X+C+a(X_1-X)^m, \qquad (X_0<X<X_1) \quad (1)$$

$$\delta=4.606X+C, \qquad (X>X_1) \quad (2)$$

with $X\equiv\log_{10}(p/m_0c)$, where p and m_0 are the momentum and the rest mass of the incident particle. In Eqs. (1) and (2), C, a, m, X_0, and X_1 are constants which are characteristic of the substance considered. Thus C is given by

$$C=-2\ln(I/h\nu_p)-1, \quad (3)$$

where I is the mean excitation potential for the electrons of the substance and $h\nu_p$ is the corresponding plasma energy, with ν_p defined by

$$\nu_p=(ne^2/\pi m_e)^{1/2}, \quad (4)$$

where n is the electron density (number of electrons per cm^3), and m_e is the electron mass. An expression for $h\nu_p$ in Rydberg units is given by Eq. (5) of Ref. 6.

We will now discuss the choice of the values for the mean excitation potential I. For all cases with $Z\geq13$ (Al, Si, Ca, I, and Cs), we used the following semi-empirical expression proposed by Sternheimer:[6]

$$I/Z=9.76+58.8Z^{-1.19}\ \text{eV}. \quad (5)$$

This gives $I=163$ eV for Al, 172 eV for Si, 228.5 eV for Ca, 545 eV for I, and 564 eV for Cs. The values for Li (39 eV), B (70 eV), O (96 eV), Ne (130 eV), and Na

* Work performed under the auspices of the U.S. Atomic Energy Commission.
[1] E. Fermi, Phys. Rev. **57**, 485 (1940).
[2] G. C. Wick, Nuovo Cimento **1**, 302 (1943).
[3] O. Halpern and H. Hall, Phys. Rev. **73**, 477 (1948).
[4] R. M. Sternheimer, Phys. Rev. **88**, 851 (1952); **91**, 256 (1953).
[5] R. M. Sternheimer, Phys. Rev. **103**, 511 (1956).
[6] R. M. Sternheimer, Phys. Rev. **145**, 247 (1966).